**M Ű E G Y E T E M 1 7 8 2**

**BME**

**Budapest University of Technology and Economics**

**Faculty of Mechanical Engineering**

**Department of Fluid Mechanics**

---

# Aerodynamic effects of blade sweep and skew applied to rotors of axial flow turbomachinery

**Ali R. A. Kwedikha**

**The Booklet of the Thesis Submitted for the Degree of Doctor of Philosophy**

**Supervisor:**

**Dr. János Vad**

**Budapest, 2009**

## 1. INTRODUCTION AND OBJECTIVES

An axial flow rotor (eg. fan) blade is backward-swept (**BSW**) or forward-swept (**FSW**) when the sections of an unswept (**USW**) datum blade of radial stacking (**RS**) line are shifted parallel to their chord in such a way that the blade section under consideration is downstream/upstream of the neighbouring blade section at lower radius. A blade is circumferentially forward skewed (**FSK**) when the sections of an unskewed (**USK**), radially stacked datum blade are shifted along the circumference toward the direction of rotation. Blade sweep, dihedral, and skew are known as techniques of non-radial blade stacking. A blade can be modified by sweep and/or dihedral if the blade sections of a datum blade of radial stacking line (**SL**) are displaced parallel to and/or normal to the chord, respectively as sketched in **Figure 1**.

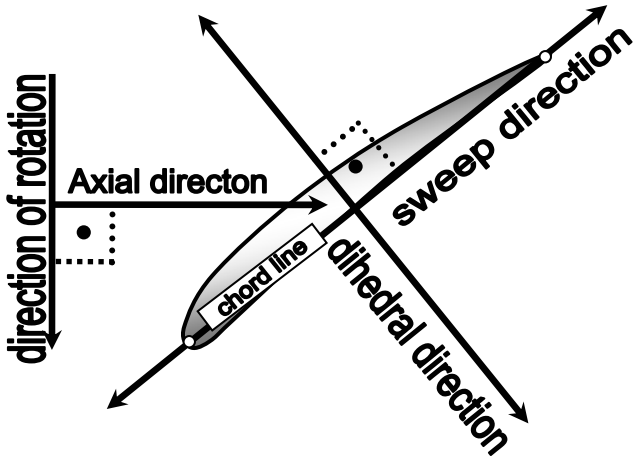


**Fig. 1. Direction of sweep and dihedral**

Sweep is said to be positive (+) or negative (-) near an endwall when a blade section under consideration is upstream or downstream of the adjacent inboard section, respectively, as outlined in **Figure 2**.

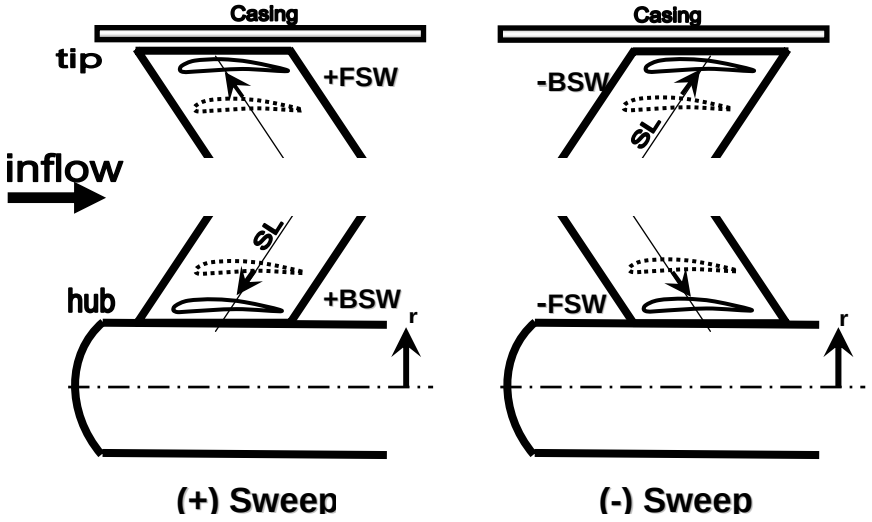


**Fig. 2. Schematic drawing for the definition of positive/negative forward and backward sweep**

By means of FSK, FSW can be incorporated in the blade geometry while the axial extension of the rotor can be retained. **Figures 3 and 4** present the comparative BSW, USW and FSW as well as USK and FSK rotors, being the subjects of present investigation.

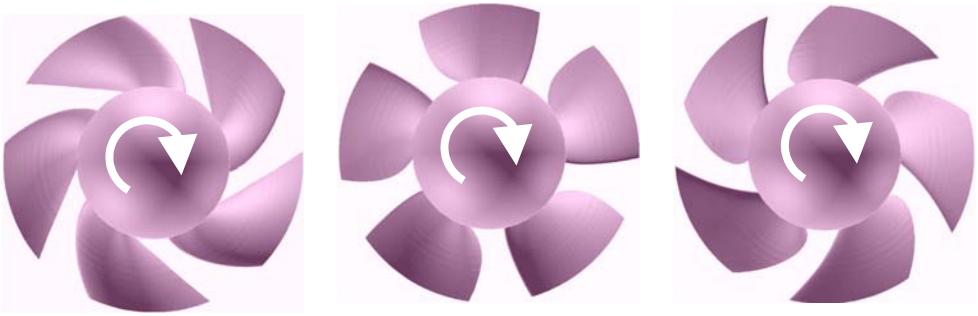


**Fig. 3. Front views of backward-swept, unswept and forward-swept rotor bladings**

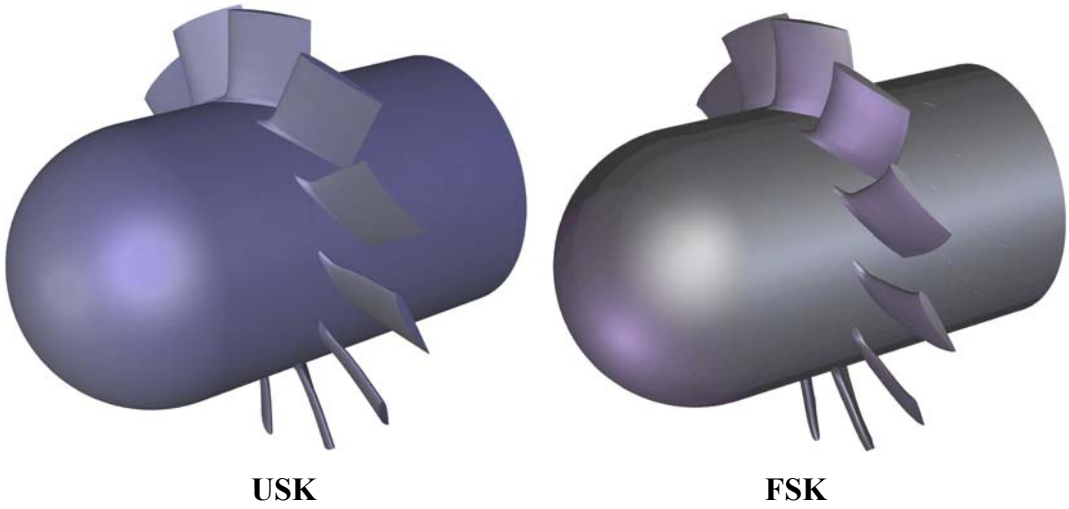


**Fig. 4. Isometric views of rotors with unskewed and forward-skewed blades**

The literature reflects a consensus that FSW or FSK give potential for the following advantages in the part load operational range (flow rates lower than design): improvement of efficiency, increase of total pressure peak, and extension of stall-free operating range by improving the stall margin (e. g. Yamaguchi et al., 1991; Beiler, 1996; Beiler and Carolus, 1999; Corsini and Rispoli, 2004; Clemen et al., 2004). Nevertheless, the research results are rather diversified regarding the judgment of performance and loss modifying effects of FSW/FSK at flow rates near the design point. In Clemen and Stark (2003), it is pointed out generally that forward sweep near the tip gives a potential for reduction of near-tip losses. Based on Yamaguchi et al. (1991), application of near-tip FSW can be recommended for efficiency improvement over the operational range near the design point. Mohammed and Prithvi Raj (1977), Beiler (1996), Beiler and Carolus (1999) and Corsini and Rispoli (2004) suggest that the application of FSW along the entire span is beneficial for loss reduction and performance improvement. However, FSK in Meixner (1995) as well as FSW reported by Clemen et al. (2004) were found to cause the deterioration of efficiency near the design point. In Kuhn (2000), the reduction of efficiency was

established for a FSW rotor over the dominant part of the entire stall-free operational range. BSW was reported by Jang et al. (2006) to be optimal from the viewpoint of efficiency improvement.

The above literature overview suggests that the performance and loss modifying effects of blade sweep and skew are not yet fully understood. The thesis work contributes to a more comprehensive understanding of aerodynamic effects of blade sweep or skew. This gives an aid to establishment of advanced concepts – being beyond the scope of the thesis – for incorporation of sweep or skew in blade design, for aerodynamic improvement of axial flow rotors.

For this purpose, two comparative case studies have been carried out, incorporating isolated axial flow rotors with swept as well as skewed blades, considered as representative examples of industrial turbomachinery rotor configurations. Incompressible flow has been assumed. The studied bladings are of relatively low aspect ratio (**AR**). This implies that sweep or skew, even if it is confined to the near-endwall regions, influences the blade aerodynamics along the entire span.

## 2. ROTOR DATA AND CASE STUDIES

### *2.1. Comparative studies on BSW, USW and FSW rotors*

The rotors depicted in **Figure 3** were preliminarily investigated at the Institute for Hydraulic Fluid Machinery, Graz University of Technology, Austria (Kuhn, 2000; Forstner, 2002). Main data of the rotors are: blade count $N = 5$; $AR = 0.56$; blade sweep angle of BSW and FSW (constant along the span): ±45°; design flow coefficient (calculated with annulus area) $\Phi_D = 0.39$; nominal total pressure coefficient $\Psi = 0.30$; Reynolds number based on tip speed and midspan chord $Re = 1.99 \cdot 10^6$.

Detailed flow measurement data on the inlet and outlet flow field were available (Kuhn, 2000), incorporating total pressure and velocity measurements. These data have been further processed during the thesis work in a purposeful manner, by means of cascade theory. Blade section lift and drag coefficients ($C_L$, $C_D$), lift-to-drag ratio (**LDR**), total efficiency ($\eta$), and Lieblein diffusion factor ($D$) have been derived and evaluated along the blade span. This added to the originally available literature database containing the axial flow as well as ideal and real total pressure rise coefficients. The studies have considered a number of operating points in the part-load range (flow rates lower than design, also including the stalled range), near the design point, and in the overload range (flow rates higher than design).

This work is considered as a supplement to the open literature on sweep effects, having the following limitations:

- The reports are often confined to the comparison of a single swept case study blading with an unswept datum blading (Lee and Baek, 2003; Xu and Amano, 2004; Braun and Seume, 2006; Lotfi et al. 2006).
- Sweep is often confined to the vicinity of one endwall, e. g. the tip region, if the endwall loss is intended to be controlled by means of sweep (Clemen and Stark, 2003). Such studies have limited relevance to judge the effects of sweep when it is applied along the entire span, e. g. for certain fan applications.

- The comparison between swept and unswept datum bladings often regards only one operating state or only a few operating points (Yamaguchi et al., 1991; Corsini and Rispoli, 2003).
- The AR of the reported bladings is relatively high (Smith and Yeh, 1963; Helming, 1996). The conclusions of such studies can be applied only with limitations to low AR bladings, applied e. g. in high-pressure industrial fans and pumps. For such cases, the blade sweep, even if it is confined to the near-endwall region, affects the flow strongly along the entire span.
- The traditional force coefficients such as blade lift and drag coefficients are used even nowadays for characterisation of turbomachinery blades (Clemen and Stark, 2003; Clemen et al., 2004; Horlock and Denton, 2005). However, the literature lacks in processing measurement data on swept blades in order to provide blade lift and drag coefficients, characterising blade load and losses in a comprehensive and lifelike manner.

### *2.2. Comparative studies on USK and FSK rotors*

These rotors, shown in **Figure 4**, were designed at the Department of Fluid Mechanics, BME. The FSK version has been installed and is under operation in the open-type low-speed wind tunnel facility of the Hungarian Institute of Agricultural Engineering, Gödöllő, Hungary. Main data of the rotors are: $N$ = 12; $AR$ = 1.08; blade skew angle of FSK (varying along the span): 0 to 3.5°; $\Phi_D = 0.33$; $\Psi = 0.27$; $Re = 1.07 \cdot 10^6$.

After a detailed analysis of a wide operational range for the swept-bladed rotors, the studies on USK and FSK were confined to the design point. In order to obtain information on the interblade flow details, a Computational Fluid Dynamics (**CFD**) technique has been developed, using the finite-volume CFD code FLUENT. The CFD tool was validated for the design point using the measurement data obtained in the Gödöllő facility. **Figure 5** shows the real and "virtual" FSK rotors (the latter was used in the CFD analysis).

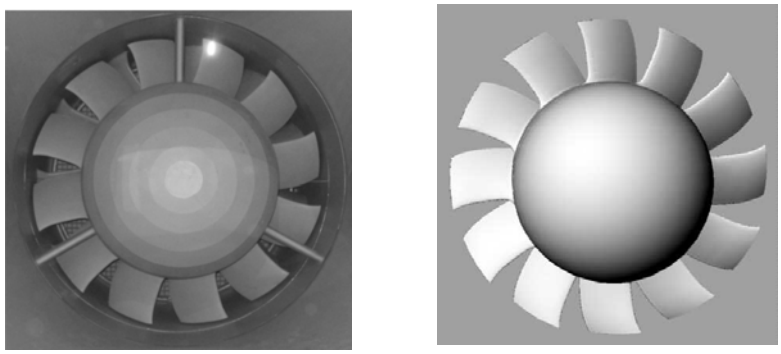

**Real FSK rotor** **Virtual FSK rotor**

**Fig. 5. Front view of real and virtual FSK rotors**

## 3. RESULTS AND DISCUSSION

### *3.1. Studies on the effects of blade sweep*

The effects of BSW and FSW (**Figure 3**) on the local performance and loss behaviour have been investigated in the vicinity and also farther from the endwalls. These investigations have been compared to the datum rotor of USW blading. To the author's best knowledge, this work is the first one publishing experiment-based data on spanwise distributions of total efficiency, profile lift and drag, and Lieblein diffusion factor in low aspect ratio subsonic rotors of various blade sweeps.

- ***Characteristic and total efficiency curves***

The characteristic and efficiency curves are shown in **Figure 6.** FSW has the broadest stall-free operational range (the peak pressure point is at the lowest flow rate), and its efficiency is the highest at near-minimum flow rates of the investigated range. This is in accordance with the general view on the benefits of FSW. However, FSW shows the lowest efficiency near the design point. The reason for this behaviour will be explained later.

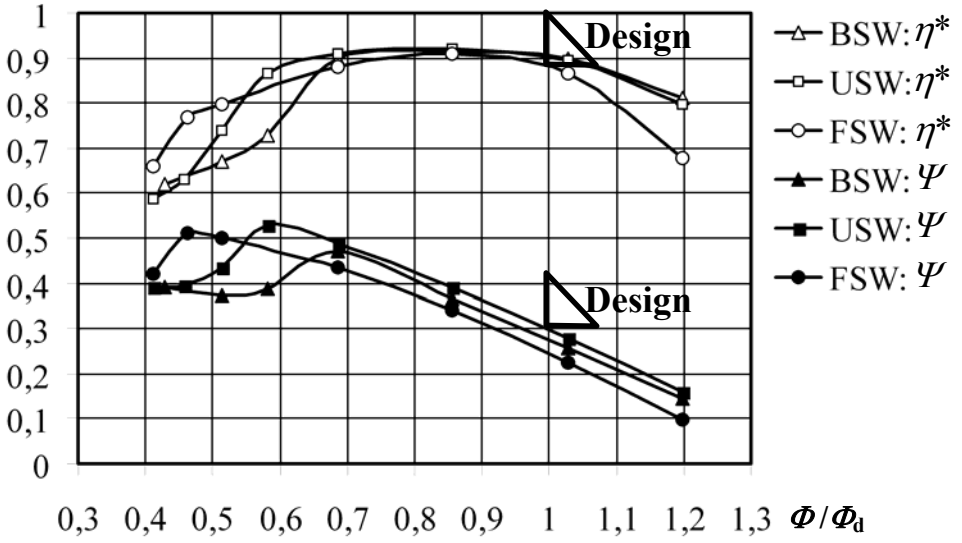


**Fig. 6. Characteristic and efficiency curves**

- ***Lift coefficient***

The lift coefficient $C_L$ is used herein as a synthetic indicator of aerodynamic load of the turbomachinery blade sections. Publications by Clemen and Stark (2003), Clemen et al. (2004) and Horlock and Denton (2005) confirm the usefulness of such an interpretation. **Figure 7** presents the spanwise distribution of lift coefficient at the design flow rate. Sweep is said to be negative [**(-)SW**] or positive [**(+)SW**] near an endwall if the blade section under consideration is downstream or upstream of the adjacent inboard blade section, respectively. This implies that the BSW and FSW rotors have (-)SW near the tip and hub, respectively. Furthermore, the BSW and FSW rotors have (+)SW near the hub and tip, respectively.

In the theoretical work by Clemen and Stark (2003) considering inviscid fluid, the blade section lift coefficient is used for characterisation of local blade load changes due to sweep. Their studies suggest that the lift coefficient tends to decrease and increase due to (+)SW and (-)SW, respectively, with regard to the unswept datum blading. The data in **Figure 6** are in agreement with these trends. Relative to USW, BSW yields decreasing $C_L$ values near the hub [(+)SW]. Near the tip of BSW [(-)SW], $C_L$ valid for USW tends to be retained or even increased. Just the opposite trends can be observed for FSW: retained $C_L$ near the hub [(-)SW], decreased $C_L$ near the tip [(+)SW]. Work by a number of researchers also suggest the unloading/uploading effect of (+)SW/(-)SW, reporting on local blade performance parameters such as axial velocity and total pressure rise, instead of $C_L$ (Shang et al., 1993; Helming, 1996; Sasaki and Breugelmans, 1998; Friedrichs et al., 2001; Gümmer et al., 2001).

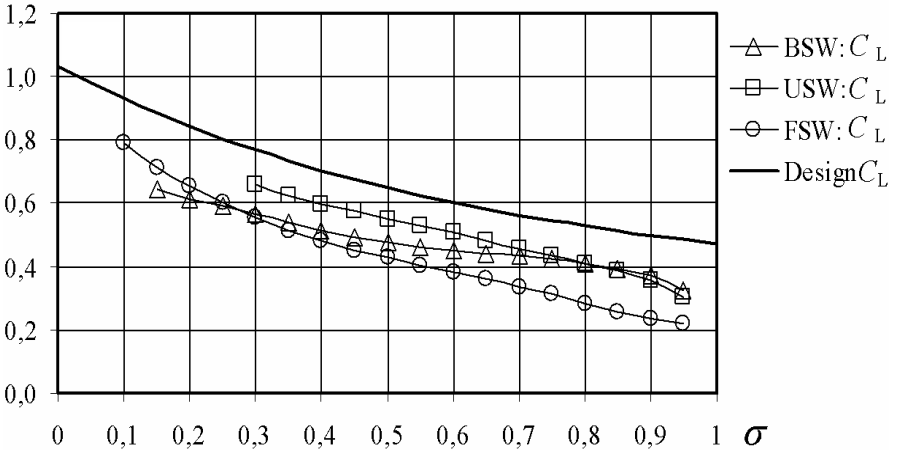


**Fig. 7. Spanwise distributions of local lift coefficient at the design flow rate**

**Figure 8** presents the characteristics of lift coefficient as function of flow rate at near-hub, near-midspan and near-tip locations. At part load, especially at near-stall and stalled conditions ($\Phi < 0.7\ \Phi_D$), the $C_L$ data for FSW tends to be higher than those for USW and BSW, along the entire span. This indicates the benefit of FSW in improvement of stall margin (eg. Yamaguchi et al., 1991), observed in **Figure 6**. Therefore, $C_L$ has been found as an appropriate indicator of blade loading capability also at part-load.

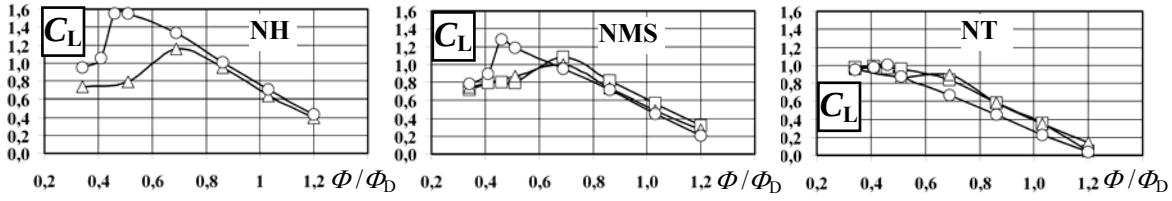


**Fig. 8. Local lift coefficient vs. flow rate at near-hub, near-midspan and near-tip locations**
NH: near-hub, NMS: near-midspan, NT: near-tip. Triangles: BSW, squares: USW, circles: FSW.

- ***Lift-to-drag ratio***

**Figure 9** presents the spanwise distribution of lift-to-drag ratio (**LDR**) at the design flow rate. According to the view represented by Clemen and Stark (2003), (+)SW, i.e. FSW near the tip, gives potential for loss reduction. As was discussed before, (+)SW also causes the reduction

of load. As the figure shows, FSW performs the lowest LDR along the dominant part of span, also near the tip where (+)SW applies.

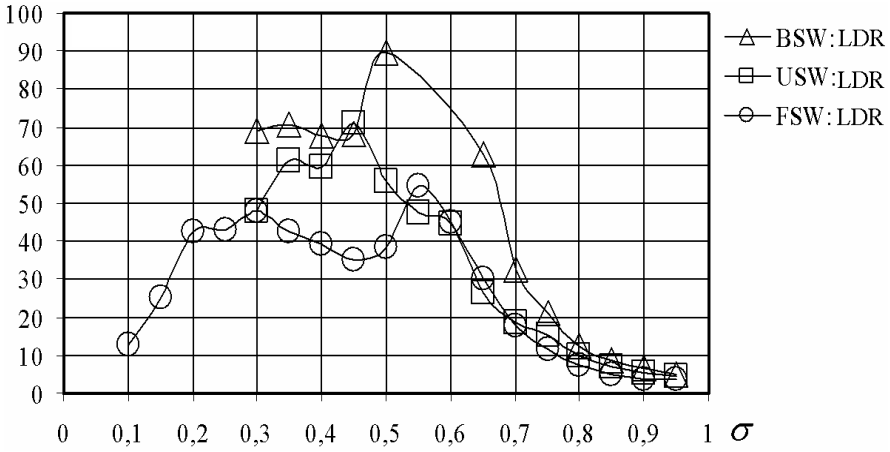


**Fig. 9. Spanwise distributions of lift-to-drag ratio at the design flow rate**

- ***Total efficiency***

**Figure 10** shows the local total efficiency profiles at the design flow rate along the span. Being consistent with the comments on the LDR, the FSW rotor exhibits the lowest efficiency along the entire span, especially near the tip, where the aerodynamic benefits of (+)SW would be expected on the basis of Clemen and Stark (2003). This calls the attention that in the aerodynamic evaluation of sweep, i.e. in modification of performance and efficiency, the balance of modification of both blade load and loss due to sweep are to be considered. This can be carried out by means of appropriate CFD tools. In the investigated case, FSW near the tip, i.e. (+)SW, was found to reduce both the load (represented by the lift) and the loss (represented by the drag) at the tip, but the reduction of load dominates over that of the loss, causing eventually the deterioration in local efficiency.

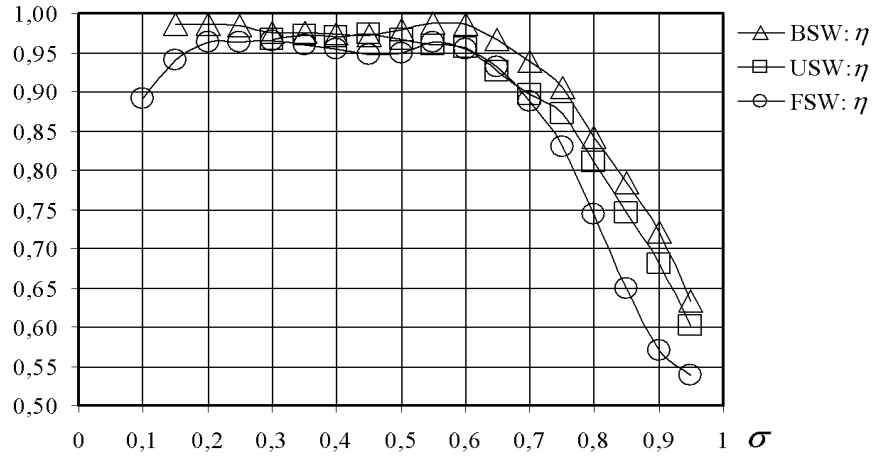


**Fig. 10. Spanwise distributions of local total efficiency at the design flow rate**

**Figure 11** presents the local total efficiency as a function of flow rate. The figure indicates that the favourable effect of FSW at the lowest flow rates, i.e. improvement of total efficiency, extends to the entire span, including even the near-hub region featuring (-)SW, from which less favourable aerodynamic behaviour may be expected on the basis of Clemen and Stark (2003).

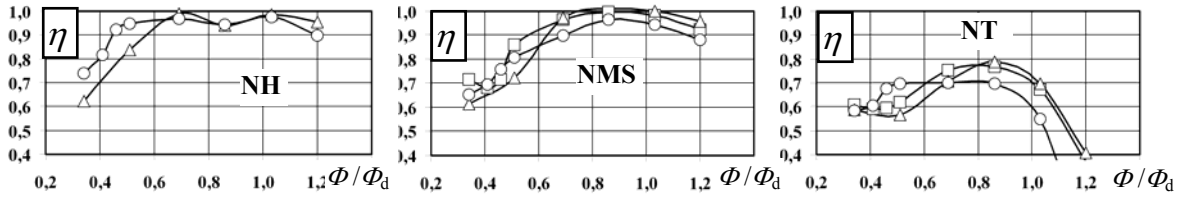


**Fig. 11. Local total efficiency vs. flow rate at near-hub, near-midspan and near-tip locations**
NH: near-hub, NMS: near-midspan, NT: near-tip. Triangles: BSW, squares: USW, circles: FSW.

- ***Lieblein diffusion factor***

The Lieblein diffusion factor $D$ (Lieblein, 1965) is considered in preliminary blade design as a criterion to avoid excessive diffusion leading to increased losses (e. g. Kuhn, 2000). The Lieblein diffusion factor $D$ is defined as follows (Lieblein**,** 1965):

$$D = \left(1 - \frac{\sin\beta_1}{\sin\beta_2}\right) + \frac{\sin\beta_1}{2(c/s)}\left(1/\tan\beta_1 - 1/\tan\beta_2\right)$$

The literature lacks $D$ distributions based on measurements in swept-bladed rotors. **Figure 12** shows the characteristics of measurement-based Lieblein diffusion factor along the span, at the design flow rate. **Figure 13** presents the dependence of $D$ on the flow rate, at three spanwise positions. Comparing **Figures 7** and **8** to **Figures 12** and **13**, it is noted that the sweep-related trends of $C_L$ and $D$ are similar. As **Figure 12** suggests, in the near-hub region of FSW [i.e. (-)SW], the trend of increased diffusion and the associated losses is properly indicated by the maximum values of $D$. Elsewhere, $D$ is generally the lowest in the case of FSW, which appears to be in contrast with the lowest LDR and efficiency. The drag was found even to be increased for FSW in certain regions away from the tip. This suggests that $D$, based on a two-dimensional cascade concept, must be treated with criticism in judgment of low-AR swept cascades from an energetic point of view in which three-dimensional flow effects are pronounced.

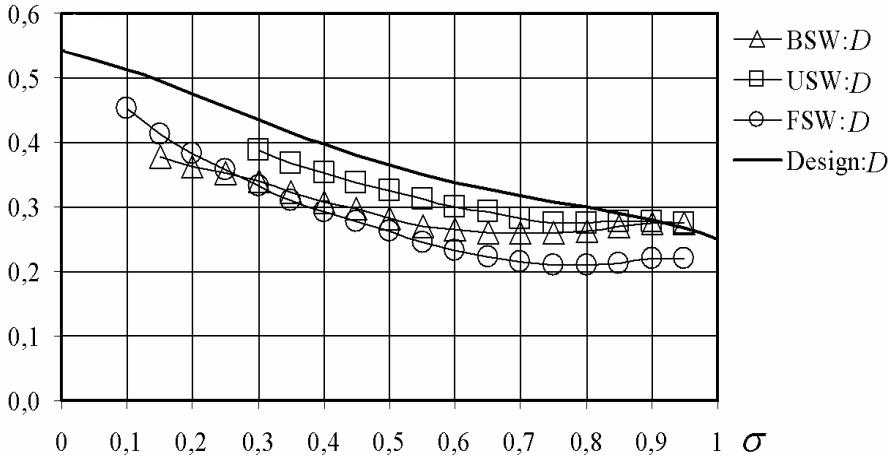


**Fig. 12. Spanwise distributions of local Lieblein diffusion factor at the design flow rate**

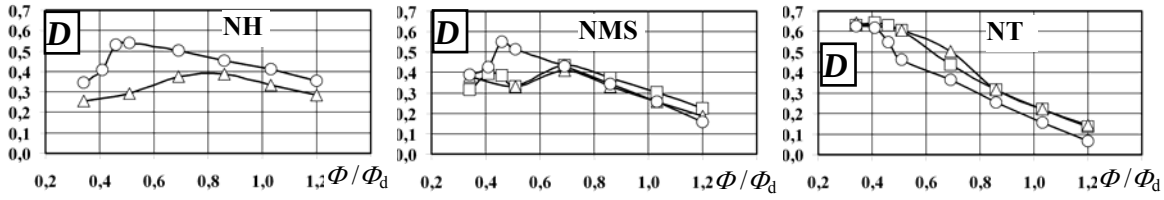


**Fig. 13. Diffusion factor vs. flow rate at near-hub, near-midspan and near-tip locations**
NH: near-hub, NMS: near-midspan, NT: near-tip. Triangles: BSW, squares: USW, circles: FSW.

### *3.2. Studies on the effects of blade skew*

- ***CFD methodology***

Referring also to **Figure 4**, **Figure 14** presents the USK and FSK blade geometries used in the CFD analysis.

It has been noted by Ferziger and Peric (2002) that structured grids are difficult or even impossible to be constructed for complex geometries. Still, it was aimed at elaborating multiblock structured grids for the rotors studied herein, for the benefits commented below. A smooth splitting scheme has been elaborated and utilized for the entire domain, applying hexahedral meshes all over the geometry. The methodology has been elaborated for CFD on axial flow rotors, as adaptation and extension of techniques suggested by Benini and Biollo (2006) and Wu et al. (2006), adding to the CFD methodology available in the open literature.

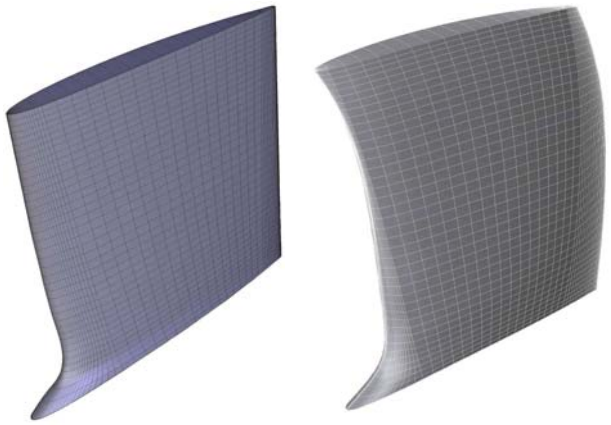

**USK** **FSK**

**Fig. 14. Isometric view of USK and FSK blades**

Comparative investigations have been carried out between single-block unstructured and multiblock structured grids on the FSK rotor. Two types of CFD techniques have been investigated:

- Single-block unstructured - 2D triangular and 3D tetrahedral-grid
- Multiblock structured - 2D quadrilateral and 3D hexahedral- grid

The chosen structured meshing technology offers the following benefits:

- By means of smooth splitting of the whole domain, complex geometries such as blading with non-radial stacking can be relatively simply handled.
- By applying the structured grid methodology, it became possible to create different block sizes separately, eg. in the tip clearance region. Such zones can be manipulated (such as grid refinement) simply and quickly, relative to unstructured grid.
- The offered moderation of cell number makes possible cost-effective CFD investigations.
- The high quality of the grid, e. g. limited cell skewness improves the quality of the computations. As example for the benefit of structured hexahedral meshing, **Figure 15** shows a comparison in resolution of the blade wake (zone indicated by an ellipse).
- The detailed results can be effectively demonstrated by using this grid. An example is presented in **Figure 16**. Here, the flow pattern can be clearly visualized by means of pathlines released only from the suction side part of blade leading edge.

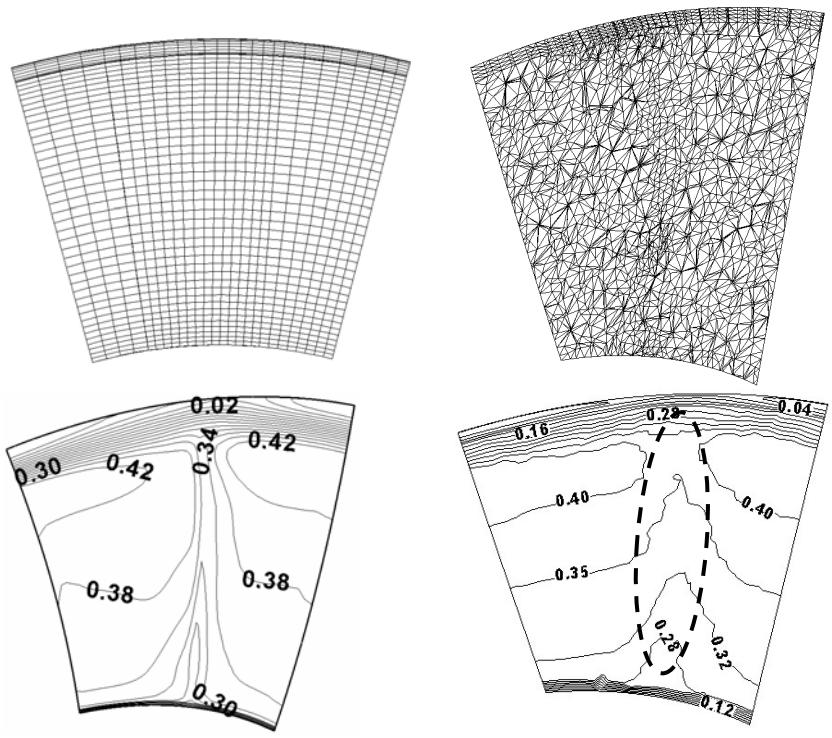


a) Structured mesh b) Unstructured mesh

**Fig. 15. Structured and unstructured meshing at outlet plane**

***Upper row: meshed outlet planes, Lower row: dimensionless axial velocity at the outlet***

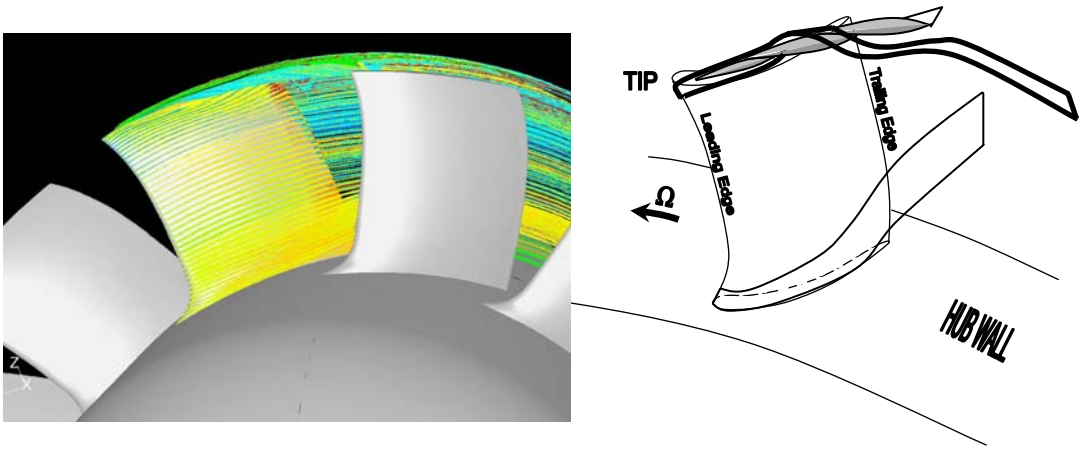


**Fig. 16. Flow visualisation using pathlines for the structured mesh.**

***Left: Pathlines released at the blade leading edge. Right: schematic representation of flow past the blade.***

- ***Comparative CFD studies on USK and FSK at the design flow rate***

Contrary to the expectations based on eg. Yamaguchi et al.(1991), introduction of FSK caused a deterioration in the overall total efficiency. The reason has been investigated in detail.

The studies on the flow field related to bladings with non-radial stacking focus on the interblade and downstream flow phenomena (e. g. Yamaguchi et al., 1991; Clemen et al., 2004). They usually report negligible effect of non-radial stacking on the upstream flow field, as in Clemen et al., (2004), probably due to the too large distance of the upstream investigation plane from the leading edge. The inlet flow field has been investigated for USK and FSK. Sufficiently closely to the leading edges (20 % chord) in the upstream flow field, the forward effect of skew has already been detected in the studies presented herein, as shown in the inlet axial velocity plots in **Figure 17**.

The trend observed in **Figure 17** has been explained as follows. The near-tip part of the forward-skewed blade protrudes into the upstream relative flow field, and carries out work in advance compared to the blade sections at lower radii. This results in locally increased inlet axial velocity near the tip. According to the conservation of mass at the prescribed design flow rate, increase of inlet axial velocity near the tip results in the reduction of inlet axial velocity at lower radii of FSK.

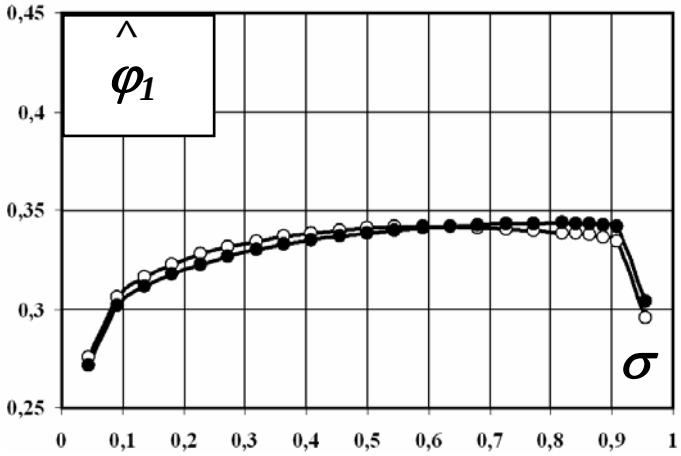


**Fig. 17. Spanwise distribution of pitchwise-averaged dimensionless inlet axial velocity**
White dots: USK, black dots: FSK

The decreased inlet axial velocity at lower radii leads to increased incidence, lift, and blade performance. Such uploading below midspan, coupled with unloading above midspan due to sweep (Smith and Yeh, 1963), modifies the Euler work distribution of the rotor along the entire span, relative to the unskewed datum rotor. This trend can be observed in the dimensionless ideal total pressure rise plots in **Figure 18**.

The increased (off-design) incidence at lower radii causes increased adverse streamwise pressure gradient on the blade suction side, leading to increased profile loss. This leads to increased total pressure loss along the dominant part of span of FSK, as shown in the total pressure loss coefficient plots in **Figure 19**.

The efficiency and performance modification of a rotor, due to introduction of FSK, depends on the balance of the aforementioned load and loss modifying effects.

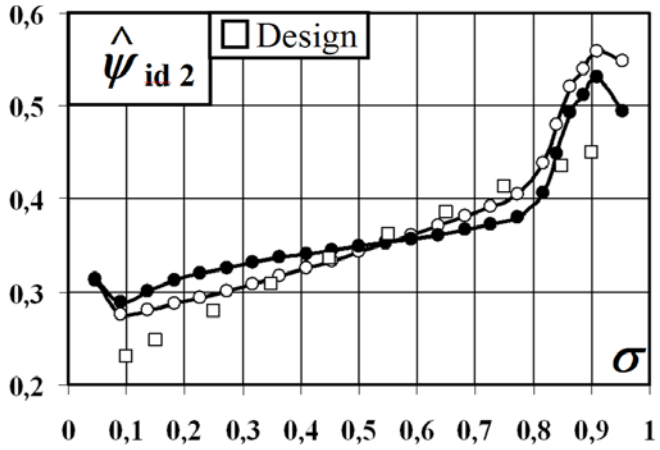


**Fig. 18. Spanwise distribution of pitchwise-averaged dimensionless ideal total pressure rise**
White dots: USK, black dots: FSK

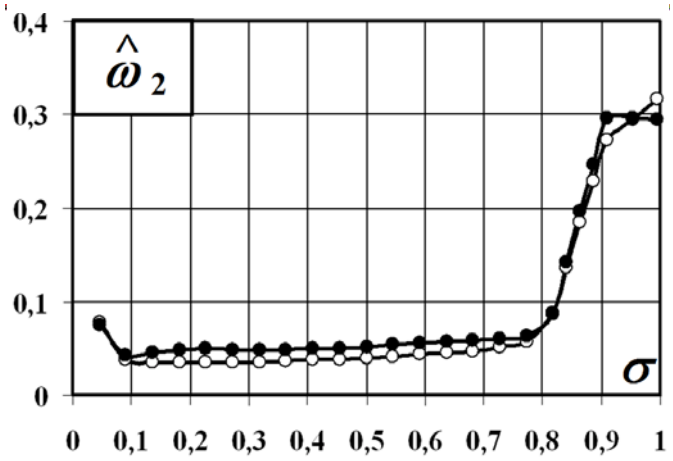


**Fig. 19. Spanwise distribution of pitchwise-averaged total pressure loss coefficient**
White dots: USK, black dots: FSK

## 4. PRACTICAL UTILIZATION OF RESULTS

The qualitative guidelines presented herein contribute to the departmental experiences on design, analysis and operation of axial flow rotors. The practical utilization is twofold:

- The results give an aid for refinement of methodology applied in ad hoc design as well as research and development (**R&D**) of axial flow industrial fans incorporating sweep or skew, in order to improve the efficiency and to realize the prescribed design point more accurately. The ad hoc design regards the preliminary design (first cut) of blading geometry. The ad hoc R&D regards the trial-and-error improvement of blade aerodynamics via iterative attempts incorporating various versions of blade geometry.
- The results can contribute to the development of an algorithmized, automated, computer-aided blade optimization methodology, such as in Lotfi et al. (2006). The most significant parameters and the appropriate parameter ranges can be identified and refined on the basis of qualitative guidelines.

## 5. THESIS POINTS

**THESIS POINT 1** Related publications: [1][5]
In the low-aspect-ratio rotors of axial flow turbomachines having swept blades, measurement-based evidence has been provided that the blade section lift coefficient $C_L$ is an appropriate indicator of local blade load modification near the endwalls due to sweep, at the design flow rate.

**THESIS POINT 2** Related publications: [1][5]
At the design flow rate, the forward-swept rotor was found to perform reduced efficiency along the entire span, especially near the tip, where, dedicated to positive sweep, just the opposite tendency was expected. Taking this example, it has been pointed out that in the aerodynamic evaluation of sweep, i.e. in modification of performance and efficiency, the balance of modification of both blade load and loss due to sweep is to be considered.

**THESIS POINT 3** Related publications: [1][5]
The sweep-related qualitative trends in the Lieblein diffusion factor $D$ and in $C_L$ were detected to be similar at the design flow rate. $D$ was found to be the lowest along a large portion of the span for the forward-swept rotor, also exhibiting the lowest lift-to-drag ratio and efficiency, as well as increased drag coefficient at certain locations. On this basis, it has been concluded that $D$ as a usual design criterion for loss reduction is to be treated with criticism, if low-aspect ratio blades with non-radial stacking are considered. The probable reason is that three-dimensional flow effects are pronounced for such bladings, whereas the $D$ criterion is based on two-dimensional cascade measurements.

**THESIS POINT 4** Related publication: [5]
At near-stall and stalled conditions, the $C_L$ data for the forward-swept rotor were found to be higher than those for the unswept and back-swept rotors, along the entire span. Therefore, $C_L$ has been qualified as an appropriate indicator of enhanced blade loading capability, at part-load.

**THESIS POINT 5** Related publication: [5]
The efficiency improving effect of forward sweep was detected along the entire span at the lowest flow rates, including even the near-hub region featuring negative sweep. The extension of load- and efficiency gaining effect of forward sweep to the entire span can be attributed to the low aspect ratio, at the lowest flow rates.

**THESIS POINT 6** Related publication: [5]
The sweep-related qualitative trends in the Lieblein diffusion factor $D$ and in $C_L$ were detected to be similar within the entire operational range under investigation.

**THESIS POINT 7** Related publications: [6][7]
Comparative CFD studies have been carried out on circumferentially forward-skewed and unskewed rotors at the design flow rate. A qualitative model has been established, contributing to the explanation of load-and loss-modifying effects. It was observed that the near-tip part of the forward-skewed blade protrudes into the upstream relative flow field, and carries out work in advance compared to the blade sections at lower radii. This results in locally increased inlet axial velocity near the tip. According to the conservation of mass at the prescribed design flow rate, increase of inlet axial velocity near the tip results in the reduction of inlet axial velocity at lower radii of the rotor.

**THESIS POINT 8** Related publications: [6][7]

At the near-field upstream of the rotor, the decreased inlet axial velocity at lower radii was found to result in increased incidence, lift, and blade performance. Such uploading below midspan, coupled with unloading due to sweep, modifies the Euler work distribution of the rotor along the entire span, relative to the unskewed datum rotor.

**THESIS POINT 9** Related publications: [6][7]

The increased (off-design) incidence at lower radii was found to cause increased adverse streamwise pressure gradient on the blade suction side, leading to increased profile loss. As a consequence, increased total pressure loss was observed along the dominant part of span of the forward-skewed rotor. The efficiency and performance modification of a rotor, due to introduction of forward skew, depends on the balance of the aforementioned load and loss modifying effects.

## PUBLICATIONS IN THE SUBJECT OF THE DISSERTATION


[1] Vad, J., Kwedikha, A. R. A., and Jaberg, H. (2004), Influence of Blade Sweep on the Energetic Behavior of Axial Flow Turbomachinery Rotors at Design Flow Rate. Proc. *2004 ASME TURBO EXPO*, Vienna, Austria, *ASME Paper* No. GT2004-53544 (CD-ROM)

[2] Vad, J., Kwedikha, A. R. A., Kristóf, G., Lohász, M. M., Rábai, G., Watanabe, K., and Rácz, N. (2005), Effects of Blade Skew in an Axial Flow Rotor of Controlled Vortex Design. Proc. *6th European Conference on Turbomachinery Fluid Dynamics and Thermodynamics (ETC'05)*, Lille, France, pp. 46-55.

[3] Vad, J., Kwedikha, A. R. A., and Rábai, G. (2005), The Effect of Circumferential Forward Skew in Axial Flow Designed for Spanwise Increasing Circulation. GÉP, LVI. Évf., 1. szám, pp. 39-47. (in Hungarian)

[4] Vad, J., and Kwedikha, A. R. A., (2006), Experimental Investigation on an Axial Flow Wind Tunnel Fan by Means of On-Site Measurements. Proc. *GÉPÉSZET'2006 Konferencia (Conference on Mechanical Engineering)*, Budapesti Műszaki és Gazdaságtudományj Egyetem, Budapest, Hungary (CD-ROM) (ISBN 963 593 465 3)

[5] Vad, J., Kwedikha, A. R. A., and Jaberg, H. (2006), Effects of Blade Sweep on the Performance Characteristics of Axial Flow Turbomachinery Rotors. *Proceedings of the Institution of Mechanical Engineers – Part A: Journal of Power and Energy*, Vol. 220, pp. 737-751.

[6] Vad, J., Kwedikha, A. R. A., and Horváth, Cs., (2006), Combined Effects of Controlled Vortex Design and Forward Blade Skew on the Three-Dimensional Flow in Axial Flow Rotors. *Proc. Conference on Modelling Fluid Flow (CMFF'06)*, Budapest, Hungary, pp. 1139-1146.

[7] Vad, J., Kwedikha, A. R. A., Horváth, Cs., Balczó, M., Lohász, M. M., and Régert, T. (2007), Combined Aerodynamic Effects of Controlled Vortex Design and Forward Blade Skew in Axial Flow Rotors. *Proceedings of the Institution of Mechanical Engineers – Part A: Journal of Power and Energy*, Vol. 221, pp. 1011-1023.

## REFERENCES


- Beiler, M. G. (1996), Untersuchung der dreidimensionalen Strömung durch Axialventilatoren mit gekrümmten Schaufeln. *Doctoral Dissertation*, Universität-GH-Siegen, VDI Verlag Düsseldorf, Reihe 7: Strömungstechnik, Nr. 298.
- Beiler, M. G., and Carolus T. H. (1999), Computation and Measurement of the Flow in Axial Flow Fans With Skewed Blades. *ASME J Turbomachinery*, Vol. 121, pp. 59-66.
- Benini, E., and Biollo, R. (2006), On the Aerodynamics of Swept and Leaned Transonic Compressor Rotors. *ASME Paper* No. GT2006-90547.
- Braun, M., and Seume J. R. (2006), Forward Sweep in a Four-Stage High-Speed Axial Compressor. *ASME Paper* No. GT2006-90218.
- Clemen, C., and Stark, U., (2003), Compressor Blades with Sweep and Dihedral: a Parameter Study. Proc. *5th European Conference Turbomachinery Fluid Dynamics and Thermodynamics*, Prague, Czech Republic, pp. 151-161.
- Clemen, C., Gümmer, V., Goller, M., Rohkamm, H., Stark, U., and Saathoff, H. (2004), Tip-Aerodynamics of Forward-Swept Rotor Blades in a Highly-Loaded Single-Stage Axial-Flow Low-Speed Compressor. *10th International Symposium on Transport Phenomena and Dynamics of Rotating Machinery (ISROMAC10)*, Honolulu, Paper No. 027. (CD-ROM Proceedings)
- Corsini, A., and Rispoli, F. (2003). The Role of Forward Sweep in Subsonic Axial Fan Rotor Aerodynamics at Design and off-Design Operating Conditions. *ASME Paper* No. GT2003-38671.
- Corsini, A., and Rispoli, F. (2004), Using Sweep to Extend the Stall-Free Operational Range in Axial Fan Rotors. *Proc. Instn Mech. Engrs, Part A, J Power and Energy*, Vol. 218, pp. 129-139.
- Ferziger, J. H., and Peric, M. (2002), *Computational Methods for Fluid Dynamics*. 3rd rev, ISBN: 978-3-540-42074-3.
- Forstner, M., Kuhn, K., Glas, W. and Jaberg, H. (2001), The Flow Field of Pump Impellers with Forward and Backward Sweep. *4th European Conference on Turbomachinery Fluid Dynamics and Thermodynamics*, Florence, Proceedings pp. 577-587.
- Forstner, M. (2002), Experimentelle Untersuchungen an vorwärts und rückwärts gepfeilten Axialpumpenschaufeln. *Ph.D. Thesis*, Technische Universität Graz, Institut for Hydraulische Strömungsmaschinen.
- Friedrichs, J., Baumgarten, S., Kosyna, G., and Stark, U. (2001), Effect of Stator Design on Stator Boundary Layer Flow in a Highly Loaded Single-Stage Axial-Flow Low-Speed Compressor. *ASME J Turbomachinery*, Vol. 123, pp. 483-489.
- Gümmer, V., Wenger, U., and Kau, H.-P. (2001), Using Sweep and Dihedral to Control Three-Dimensional Flow in Transonic Stators of Axial Compressors. *ASME J Turbomachinery*, Vol. 123, pp. 40-48.

- Helming, K. (1996), Numerical Analysis of Sweep Effects in Shrouded Propfan Rotors. *J. Propulsion Power*, Vol. 12, pp. 139-145.
- Horlock, J. H., and Denton, J. D. (2005), A Review of Some Early Design Practice Using Computational Fluid Dynamics and a Current Perspective. *ASME J Turbomachinery*, Vol. 127, pp. 5-13.
- Jang, C.-M., Samad, A., and Kim, K.-Y. (2006), Optimal Design of Swept, Leaned and Skewed Blades in a Transonic Axial Compressor. *ASME Paper* No. GT2006-90384.
- Kuhn, K. (2000), Experimentelle Untersuchung einer Axialpumpe und Rohrturbine mit gepfeilten Schaufeln. *Ph.D. Thesis*, Technische Universität Graz, Institut for Hydraulische Strömungsmaschinen.
- Lee, G, and Baek, J. (2003), A Comparative Study of Turbulence Models for the Prediction of Tip Leakage Flow in Axial-Flow Turbomachinery. Proc. *Conference on Modelling Fluid Flow* (CMFF'03), Budapest, Hungary, pp. 925-932.
- Lieblein, S. (1965), Experimental Flow in Two-Dimensional Cascades. Chapter VI in *Aerodynamic Design of Axial-Flow Compressors*. NASA SP-36, Washington D. C.
- Lotfi ,O., Teixeira, J.A., Ivey, P.C., Kinghorn, I.R., and Sheard A.G. (2006), Shape Optimisation of Axial Fan Blades Using Genetic Algorithms and a 3D Navier-Stokes Solver. *ASME Paper* No. GT2006-90659.
- Meixner, H. U. (1995), Vergleichende LDA-Messungen an ungesichelten und gesichelten Axialventilatoren. *Dissertation Universität Karlsruhe*, VDI-Verlag, Reihe 7: Strömungstechnik, No. 266, Düsseldorf.
- Mohammed, K. P., and Prithvi Raj, D. (1977), Investigations on Axial Flow Fan Impellers With Forward Swept Blades. *ASME J Fluids Engineering*, September 1977, pp. 543-547.
- Sasaki, T., and Breugelmans, F. (1998), Comparison of Sweep and Dihedral Effects on Compressor Cascade Performance. *ASME J Turbomachinery*, Vol. 120, pp. 454-464.
- Shang, E., Wang, Z. Q., and Su, J. X. (1993), The Experimental Investigations on the Compressor Cascades With Leaned and Curved Blade. *ASME Paper* No. 93-GT-50.
- Smith, L. M., and Yeh, H. (1963), Sweep and Dihedral Effects in Axial-Flow Turbomachinery. *ASME J Basic Engineering*, Vol. 85, pp. 401-416.
- Wu, Y., Chu, W., Lu, X., and Zhu, J. (2006), Behavior of Tip Leakage Flow in an Axial Compressor Rotor. *ASME Paper* No. GT2006-90399.
- Xu, C., and Amano, R. S. (2004), Numerical Prediction of Swept Blade Aerodynamic Effects. *ASME Paper* No. GT2004-53008.
- Yamaguchi, N., Tominaga, T., Hattori, S., and Mitsuhashi, T. (1991), Secondary-Loss Reduction by Forward-Skewing of Axial Compressor Rotor Blading- Proc. *Yokohama International Gas Turbine Congress*, Yokohama, Japan, pp. II.61-II.68.

**List of symbols**

| | |
|---|---|
| $c$ | blade chord |
| $\beta$ | flow angle (measured from circumferential direction) |
| $\omega$ | total pressure loss coefficient = $\psi_{id}$ - $\psi$ |
| $\sigma$ | fraction of span (radial distance from the hub divided by blade span) |
| $d_h$ | blade hub diameter |
| $d_t$ | blade tip diameter |
| $S$ | blade span = $(d_t - d_h)/2$ |
| $n$ | rotor speed (in revolutions per second) |
| $u_t$ | blade tip velocity = $d_t \pi n$ |
| $Re$ | Reynolds number (based on $u_t$, midspan blade chord and fluid kinematic viscosity) |
| $\Phi$ | flow coefficient (annulus area-averaged axial velocity divided by $u_t$) |
| $\Phi_D$ | design flow coefficient |
| $v_x$ | absolute axial velocity (*m/s)* |
| $v_u$ | absolute tangential velocity (*m/s)* |
| $\varphi$ | local flow coefficient = $v_x / u_t$ |
| $\eta$ | local total efficiency = ratio between the local total pressure rise and the ideal local total pressure rise |
| $\eta^*$ | global total efficiency (product of volume flow rate and mass-averaged total pressure rise in the annulus per shaft input power) |
| $\Psi$ | global total pressure coefficient (annulus mass-averaged total pressure rise divided by $\rho u_t^2/2$) |
| $\psi$ | local total pressure rise coefficient = $\Delta p_t / ( \rho u_t^2/2)$ |
| $\psi_{id}$ | local ideal total pressure rise coefficient = $\Delta p_{t\,id} / ( \rho u_t^2/2) = 2R v_{u2}/u_t$ |

**Subscripts and Superscripts**

| | |
|---|---|
| ^ | pitchwise averaged value |
| 1 | inlet plane |
| 2 | exit plane |